Original Research

Study on the Adsorption Behavior of Cadmium by the MPs and Its Environmental Factors

Sha Wang[1], Xiaoli Wang[1], Xiaobing Wang[1, 2]*, Zhentian Qin[1], Jiale Hu[1], Sujun Ding[1], Ke Feng[1, 2]

[1]College of Environmental Science and Engineering, Yangzhou University, Yangzhou, Jiangsu 225127, China
[2]Jiangsu Organic Solid Waste Resources Collaborative Innovation Center, Nanjing, Jiangsu 210095, China

Abstract

This work examined the adsorption mechanism of microplastics made of polypropylene (PP), polyethylene (PE), and polyvinyl chloride (PVC) on Cd^{2+} and its effects on the environment. The findings demonstrated that microplastics' crystallinity and unique functional groups also affected the adsorption of Cd^{2+}, besides being a critical factor regulating the particle size of the MPs. The three MPs' Cd^{2+} adsorption kinetics conformed to the quasi-secondary kinetic model, confirming that the adsorption was nonlinear. Besides, the three MPs' Cd^{2+} isothermal adsorption process can be adequately described by the Langmuir and Freundlich models, demonstrating that monolayer and multilayer adsorption coexist and are heterogeneous adsorption processes. As indicated by the findings of the energy spectrum study, PVC (0.78%), PP (0.25%), and PE (0.18%) exhibited the maximum concentrations of Cd^{2+} adsorbed in MPs. As revealed by the findings of the effect of environmental conditions on the adsorption of Cd^{2+} by the MPs, the three MPs exhibited the maximum adsorption capacity at 35ºC and a pH of 6.0. The equilibrium adsorption of Cd^{2+} by PP, PE, and PVC was reduced by 3.3, 8, and 13 times, respectively, compared with no salt at a salt concentration of 1 mg/L salt solution.

Introduction

Plastic items have been extensively employed and have integrated seamlessly into people's lives on a day-to-day basis. 3% of all consumer goods are currently made of plastic with the invention of synthetic polymers [1]. Plastic product has been causing increasingly significant contamination of freshwater ecosystems and terrestrial habitats [2, 3], and plastics in the natural environment degrade into microplastics under the effects of mechanical corrosion, solar radiation, and biological degradation. Microplastics (MPs) refer to plastics with a particle diameter of less than 5 mm, which exhibit small particle sizes, large specific surface areas, high surface hydrophobicity, as well as weak photodegradation ability. It is noteworthy that the particle size of plastic degradation is less than 100 nm, whereas plastics on the nanoscale are difficult to detect [4]. Besides, the United Nations listed microplastic contamination as one of

*e-mail: xbwangll@hotmail. com

the top 10 environmental issues worldwide in 2014 [5]. The issue of microplastic pollution has been arousing the attention of a growing number of countries. Since pollutants adsorbing onto the surface of the MPs serve as the primary source of their environmental toxicity [6], MPs are considered the possible persistent pollutants in the environment [7]. For the first time, Leslie [8] et al. reported the presence of the MPs in human blood on March 24, 2022. The above-mentioned particles may have originated derived from plastic objects employed in people's daily lives. Nowadays, MPs are extensively spread in a variety of ecosystems (e.g., marine, terrestrial, and freshwater). Notably, the environmental harm arising from the MPs has posed a risk to people's health.

The movement and transformation of pollutants in the environment are affected by the presence of the MPs, which are pollutants and may cover heavy metals, antibiotics, and organic pollutants [9, 10]. MPs can serve as carriers to adsorb heavy metals for their high affinity in coexisting metal ions, which has been confirmed in existing research on MPs and heavy metal adsorption. Tang [11] investigated the adsorption of Pb, Cu, and Cd on polyamide-6 MPs. As indicated by their results, the descending fast and slow order of adsorption of metal ions to polyamide-6 MPs is expressed as Pb>Cu>Cd. V. Godoy [12] has suggested that PE, PP, PS, and PVC are capable of quickly adsorbing Cr, Cu, Co, and Pb since the roughness and irregularity of the microplastic surface provide considerable adsorption sites for heavy metal ions. The adsorption of heavy metals by the MPs is affected by a considerable number of factors. For instance, the type, particle size, aging degree, pH, temperature, and salinity [13-15] of the MPs will exert a certain effect on their adsorption capacity. C. Marisa [13] and Wang [16] explored the adsorption of Cd, Cu, and Pb on aging MPs. Their results suggested that the aging behavior of the MPs will change the surface characteristics of the MPs while affecting the adsorption performance of the MPs.

The existing research on the adsorption of heavy metals by the MPs has placed a major focus on the comparison of different heavy metal adsorption capacities. Nevertheless, the adsorption capacity and factors of different microplastic characteristics on Cd^{2+} are unclear, and the research on characterization techniques, mechanisms, and their environmental effects is not exhaustive. In this experiment, three common MPs-PP, PE, and PVC-were selected, and the primary research is elucidated as follows. 1. The three MPs' adsorption capacities for different particle sizes were compared. 2. The physical characteristics of various MPs and their Cd^{2+} heavy metal adsorption capabilities were evaluated. 3. The adsorption mechanism of the MPs on Cd^{2+} was examined by investigating kinetics, environmental effect factors, surfaces, and performance analysis.

Materials and Methods

Experimental Materials

Three microplastics -polyethylene (PE), polypropylene (PP), and polyvinyl chloride (PVC) -were used in the experiment, and their average particle sizes were, respectively, 154 μm, 48 μm, 30 μm, and 13 μm, all of which originated from Huachuang Plasticization Co., Ltd. (Dongguang, Guangzhou Province, China). MPs were cleaned three times with 5% nitric acid ultrasound and then washed twice with pure water. The cleaned MPs were protected from light and then air-dried naturally in plastic bags for subsequent application.

Characterization of MPs

The charge on the surface of the MPs was determined using a zeta potentiometer. The specific surface area and pore size of the MPs were determined using the Autosorb IQ3 surface area analyzer (USA). The surface functional groups of the MPs before and after Cd adsorption were determined using a Fourier transform infrared spectrometer (FTIR, Cary610/670, USA Varian). The crystalline minerals on the surface of the MPs were analyzed using X-ray diffraction (XRD, D8 Advance, and German Bruker AXS). The surface morphology and elemental content of the MPs were observed through scanning electron microscopy (SEM-EDS, HITACHI, S-4800, Japan).

Effect of Microplastic Particle Size on Cd^{2+} Adsorption

Weigh 0.05 g of four MPs with particle sizes of 13 μm, 30 μm, 48 μm and 154 μm in an Erlenmeyer flask, add 30 mL of a 10 mg/L cadmium nitrate solution, and bring the reaction system's pH to 6.5. Shake at 160 r/min for 24 h at 25ºC. After shaking, aspirate 5 mL of the supernatant with a disposable syringe, filter through a 0.22 μm needle filter, and then dilute with 1% nitric acid to control the concentration of Cd^{2+} in the solution to be measured in the detection limit of the single-flame atomic absorption spectrometer. Lastly, the content of Cd^{2+} in the filtrate was determined with a single-flame atomic absorption spectrometer (AAS, iCE 3300-Thermo, Germany). The respective set of samples was set in three parallel sets.

Experiments on Adsorption of Cd^{2+} by MPs

Adsorption Kinetic Experiments

150 mL of a 10 mg/L (in terms of Cd^{2+}) cadmium nitrate solution was added into an Erlenmeyer flask supplemented with 0.25 g of the MPs. Next, 0.01 mol/L HNO_3 and 0.01 mol/L NaOH were added to the reaction system to increase the pH to 6.5. The sample was placed

in a thermostatic oscillator with a temperature setting of 25ºC at a speed of 160 r/min. 5 mL of supernatant was aspirated with a disposable syringe at 15, 30, 60, 120, 180, 240, 480, 960, 1200, 1440, and 1920 min, filtered with a 0.22 μm needle filter, and then diluted with 1% nitric acid to control the concentration of Cd^{2+} in the solution to be examined in the detection limit of the single-flame atomic absorption spectrometer. Lastly, the content of Cd^{2+} in the filtrate was determined with a single-flame atomic absorption spectrometer (AAS, iCE 3300-Thermo, Germany). The respective set of samples was set in three parallel sets.

Adsorption Isotherm Experiment

A 100 mg/L Cd^{2+} stock solution was prepared with cadmium nitrate tetrahydrate, and a cadmium nitrate solution with a concentration of 2, 5, 10, 15, 20, 25, and 40 mg/L was prepared with a 1% nitric acid stock solution. 0.01 mol/L HNO_3 and 0.01 mol/L NaOH should be used to bring the pH of the Cd^{2+} solution to 6.5 to prevent heavy metal ion precipitation. Weigh 0.05 g of the MPs in an Erlenmeyer flask and add 30 mL of cadmium nitrate solutions of different concentrations. The method of filtration determination at 160 rpm at 25ºC for 24 h was the same as the 2.4.1 test. The respective group of processing settings was set in three parallels.

Environmental Factors of the MPs on Cd^{2+} Adsorption

Effect of Solution pH

The pH value of pure water was regulated to 3, 4, 5, 6, and 7 with 0.01 mol/L HNO_3 and 0.01 mol/L NaOH, and the heavy metal ion reserve solution was diluted with the prepared solution. Subsequently, a Cd^{2+} ionic aqueous solution with different pH values was prepared. Weigh 0.05 g of the MPs in a 50 mL Erlenmeyer flask and add 30 mL of cadmium nitrate solution with a pH of 10 mg/L. The method of filtration determination at 160 rpm at 25ºC for 24 h was the same as the 2.4.1 test. The respective group of processing settings was set in three parallels.

Effects of Solution Temperature

0.05 g of the MPs was weighed in an Erlenmeyer flask, and 30 mL of a 10 mg/L cadmium nitrate solution was added. The reaction system's pH was set to 6.5. It was placed in a thermostatic oscillator to oscillate, and the temperature of the thermostatic oscillator was set to 15, 25, 35, and 50ºC, respectively. It oscillated at 160 rpm for 24 h, and the filtration determination method after the end of the oscillation was identical to the 2.4.1 test. The respective group of processing settings was set in three parallels.

Effects of Solution Salinity

Na^+ solutions with concentrations of 0.01, 0.1, and 1.0 mg/L were prepared with NaCl, and Cd^{2+} ion stock solutions were diluted with this solution. Prepare Cd^{2+} ionized aqueous solutions of different salinities. Weigh 0.05 g of the MPs in an Erlenmeyer flask and add 30 mL of 10 mg/L cadmium nitrate solution. The method of filtration determination at 160 r/min at 25ºC for 24 h was the same as the 2.4.1 test. The respective group of processing settings was set in three parallels.

Statistical Analysis

Excel software is used for data statistics, SPSS 23.0 software is used for statistical analysis of data, and data analysis is tested by a one-way ANOVA model. The fitting and mapping of the adsorption model were performed using OriginPro 9.1 software. The adsorption capacity of Cd is calculated in Equation (1), where q_e is the adsorption amount (mg/g), C_0 is the initial concentration of Cd^{2+} (mg/L), Ce is the equilibrium concentration of Cd^{2+} at equilibrium (mg/L), V is the volume of solution (L), and m is the number of the MPs (g).

$$Q_e = V(C_0 - C_e)/m \tag{1}$$

Adsorption Kinetic Model

Quasi-first-order kinetics (PFO) and quasi-second-order kinetics (PSO) were adopted to fit the adsorption of Cd^{2+} processes in MPs, and the equations are expressed as (2) and (3):

$$\text{PFO}: Q_t = Q_e(1 - e^{-k_1 t}) \tag{2}$$

$$\text{PSO}: Q_t = \frac{Q_e^2 K_2 t}{1 + Q_e k_2 t} \tag{3}$$

Where Q_t and Q_e denote the adsorption capacities of the MPs at t time and equilibrium (mg/g), respectively; t represents the adsorption time (min); k_1 and k_2 express adsorption rate constants for PFO and PSO models, respectively.

Adsorption Isothermal Model

The Freundlich model and the Langmuir model were adopted to fit the isotherm data of the MPs adsorbing Cd^{2+}, and equations (e.g., Eq. (4) and (5)) were fitted.

$$\text{Freundlich model}: Q_e = \frac{Q_m b C_e}{1 + b C_e} \tag{4}$$

$$\text{Langmuir model}: Q_e = K_f C_e^{\,n} \tag{5}$$

Where q_e denotes the equilibrium adsorption capacity of Cd^{2+} (mg/g); C_e represents the equilibrium concentration of Cd^{2+} at equilibrium; K_F expresses Freundlich's equation constant $(mg^{1-n}/g \cdot L^n)$; n is the dimensionless constant reflecting the adsorption strength of Cd^{2+} of the adsorbent; q_m denotes the saturated adsorption capacity of Cd^{2+} in the Langmuir model (mg/g); K_L expresses the Langmuir model constant (L/mg).

Results and Discussion

Effect of Microplastic Particle Size on Adsorption of Cd^{2+}

As depicted in Fig. 1, the adsorption capacity of Cd^{2+} of the three MPs was increased with the decrease of the particle size; the equilibrium adsorption capacity of Cd^{2+} of the MPs with a particle size of 13 μm at the same concentration reached its maximum, and the PP, PE, and PVC reached 0.42 mg/g, 0.48 mg/g, and 0.56 mg/g, respectively. The MPs with a particle size of 154 μm exhibited the minimum equilibrium adsorption capacity of Cd^{2+}, with PP, PE, and PVC being 0.050 mg/g, 0.044 mg/g, and 0.049 mg/g, respectively. The equilibrium adsorption capacity of the MPs with a particle size of 13 μm was nearly 10 times that of the MPs with a particle size of 154 μm. The change in adsorption capacity was correlated with the specific surface area and adsorption site of the MPs [17]. The smaller the particle size, the larger the specific surface area of the MPs, the more adsorption sites, and the stronger the affinity for Cd^{2+}, such that the adsorption capacity of the MPs to Cd^{2+} was increased. As indicated by the above result, the adsorption capacity of metal ions on solid particles was significantly correlated with the size of the particles [18]. The material characterization,
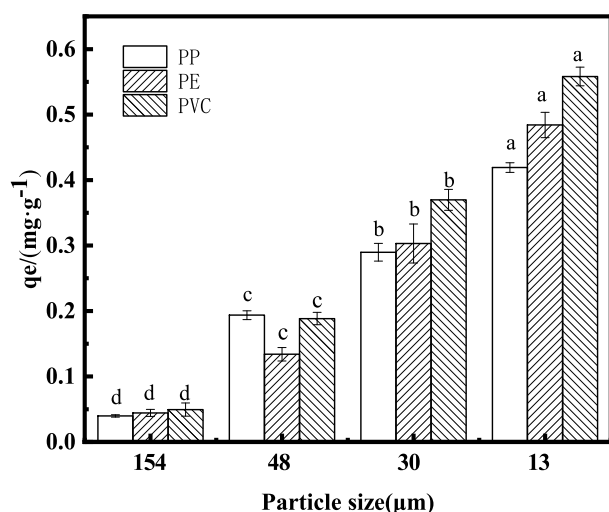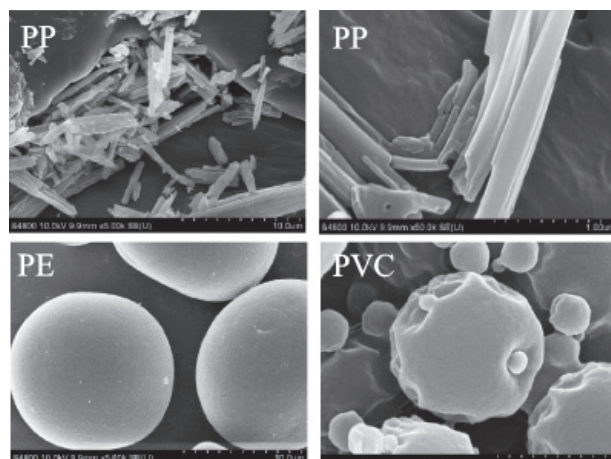

Fig. 2. SEM electron microscopy scan of the MPs.

kinetics, and environmental effects described below were all studied using the three MPs with the maximum adsorption capacity of 13 μm. Further studies were conducted with 13 μm MPs that exhibited the maximum adsorption capacity.

Material Characterization

Morphology of MPs

The microscopic morphology of the MPs was scanned through SEM electron microscopy (Fig. 2). PP is a long, fibrous debris with a smooth surface and a clear pore structure. PVC, on the other hand, is made of spherical particles of varying sizes with folds and depressions on the surface and is filled with microscopic particles. PVC is constructed of homogenous spherical particles with a smooth surface and little fissures.

Analysis of Zeta Potential

The measured Zeta potential on the surface of the MPs is negative (Table 1), while the absolute value of the ZTA potential of PVC is larger than that of both PP and PE, 3 times that of PE and 3.16 times that of PP.
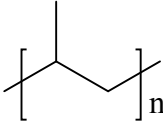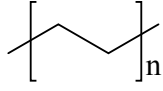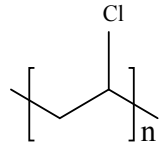
BET Analysis

The specific surface area, pore volume, and average pore size of the MPs were studied by an N_2 isothermal adsorption experiment (Table 2). The specific surface areas of PP, PE, and PVC were 0.2398 $m^2 \cdot g^{-1}$, 1.8469 $m^2 \cdot g^{-1}$, and 2.2163 $m^2 \cdot g^{-1}$, respectively. The specific surface area and pore volume of PVC are significantly larger than those of PP and PE. Specific

Fig. 1. Effect of particle size on the adsorption of Cd^{2+} by the MPs.

Table 1. Zeta potential of different MPs.

MPs	PP	PE	PVC
Zeta potential mV	-2.9±0.20a	-3.7±0.36a	-11.7±0.87b

Table 2. BET surface area and pore characteristics of the MPs.

Materials	Structure	Specific surface area (m$^2 \cdot$g^{-1})	Pore volume (cm$^3 \cdot$g^{-1})	Average pore size (nm)
PP		0.2398	0.000142	2.38
PE		1.8469	0.000976	2.13
PVC		2.2163	0.041130	74.23

surface area is one of the important parameters affecting the adsorption capacity of the MPs. In general, the larger the specific surface area, the more adsorption sites that are available, and the stronger the adsorption capacity of the MPs [19].

Surface Characteristics of MPs

EDS Analysis

Fig. 3(a, b) present the morphology and energy spectrum analysis of the PP surface before and after the adsorption of Cd. As indicated by the result of the energy spectrum analysis, the presence of Cd elements was not detected on the PP surface prior to adsorption, only C and O elements, and the Cd content were increased by 0.25% (Wt.) after adsorption, while C was decreased by 0.08% (Wt.) and O was reduced by 0.17% (Wt.). Fig. 3(c, d) illustrate the morphology and energy spectrum analysis of the PE surface before and after adsorption of Cd. The energy spectrum analysis suggested that the presence of Cd element was not detected on the PP surface prior to adsorption, only C element, and the Cd content was increased by 0.18% (Wt.) after adsorption, the O content was elevated by 1.43% (Wt.), and the C content declined by 1.61% (Wt.). Fig. 3(e, f) present the surface morphology and energy spectrum analysis of PVC before and after adsorption of Cd, and the comparative study found that the presence of Cd elements was not detected on the surface of the MPs prior to adsorption; only C elements and Cl elements existed, and the Cd content increased by 0.78% (Wt.) after adsorption. After adsorption of PP, PE, and PVC, the Cd content increased by 0.25% (Wt.), 0.18% (Wt.), and 0.78% (Wt.), respectively, and the adsorption capacity of PVC to Cd was significantly greater than that of PP and PE. Studies have shown that Cl on the surface of PVC binds to Cd through chemical bonds, which improves the adsorption capacity of Cd [20].

FTIR Analysis

The Fourier infrared spectra of the three MPs before and after Cd^{2+} adsorption (Fig. 4) and the position of the main characteristic peaks of the MPs before and after Cd^{2+} adsorption remained nearly unchanged. C-H telescopic vibration was identified in the three MPs before and after adsorption [21], PP at 2970~2853 cm^{-1}, PE at 2913~2845 cm^{-1}, and PVC at 2979~2908 cm^{-1}; hydrogen bonding was likely to serve as an adsorption mechanism for cadmium adsorption by the MPs. The peak of PP at 1712 cm^{-1} belonged to the telescopic vibration of C=C, and most of the peaks at 1405-719 cm^{-1} belonged to the telescopic vibration of C-C, where the peak at 1405 cm^{-1} belonged to the in-plane bending vibration of C-H, and the peak at 865 cm^{-1} belonged to the off-plane bending vibration of C-H. Moreover, the peak of PE at 1472 cm^{-1} belonged to the in-plane bending vibration of C-H, and the peak of 713 cm^{-1} belonged to the off-plane bending vibration of C-H. The peak of PVC at 1429 cm^{-1} belonged to the telescopic vibration of CH$_2$-CHCl, the peak at 1329~961 cm^{-1} belonged to the telescopic vibration of C-C, and the peak at 689 cm^{-1} and 613 cm^{-1} belonged to the contraction vibration of C-Cl [21].

No new chemical bonds and functional groups were formed after MPs adsorbed Cd^{2+} [22]. The major reason for this result is that the intrinsic functional groups on the surface of the MPs adsorbed heavy metals, whereas the energy intensity and peak area of the absorption peak before and after the reaction varied. The energy intensity and shape of the peak at 2970~2853 cm^{-1} before and after PP adsorption of Cd^{2+} varied, and the intensity of the peak at 1712~1405 cm^{-1} was increased after Cd^{2+} adsorption. The presence of an O element on the PP surface was detected through energy spectrum analysis, where there might be a complex reaction with cadmium. The energy intensity of the PE peak at 2913~2845 cm^{-1} was increased after Cd^{2+} adsorption. As indicated by
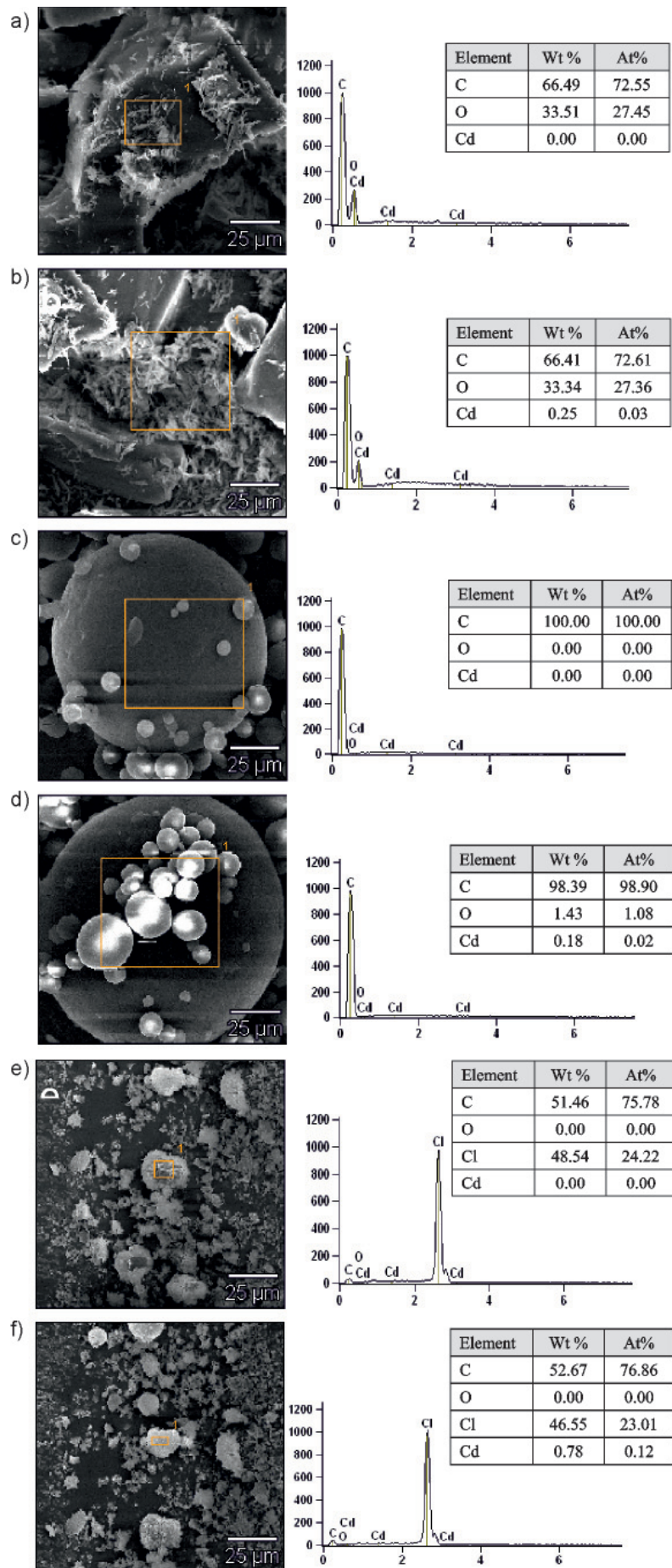
Fig. 3. EDS energy spectrum analysis before and after MPs adsorption Cd^{2+}.

the result of energy spectrum analysis, no O element was identified on the PE surface before the adsorption of Cd^{2+} and the presence of O after adsorption. Existing research has suggested that the increase of oxygen-containing functional groups may be formed through the reaction of C-H bonds on MPs with oxygen after the adsorption was broken, and the change of the above-mentioned functional groups led to the enhancement of the binding ability of the MPs to heavy metals in the environment. The intensity and energy of the peaks before and after PVC adsorption remained nearly unchanged, and no O element was reported in energy spectrum analysis, whereas the Cl atoms on the surface of PVC exhibited a high affinity for Cd^{2+}. On that basis, the adsorption of Cd^{2+} was mainly due to electrostatic attraction. The adsorption of Cd^{2+} by PP and PE might be the result of electrostatic interaction and surface complexation.

XRD Analysis

XRD spectra before and after the adsorption of Cd^{2+} by three MPs (Fig. 5) indicated the diffuse amorphous diffraction peaks before PE adsorption, and there were two fine and pointed crystalline phase diffractions. In general, polymers with significant fine and pointed diffraction peaks exhibited higher crystallinity. PP spectra showed amorphous diffraction peaks; the diffraction peaks of PVC spectra were not very significant compared with PP and PE. The higher the crystallinity of the MPs, the fewer disorderly-arranged regions, the lower the surface activity, and the weaker the adsorption capacity of heavy metals. The crystallinity order of the MPs was determined as PE>PP>PVC using Jade 6.5, consistent with EDS experimental results. As indicated by the result, the characteristic peak morphology and peak position of
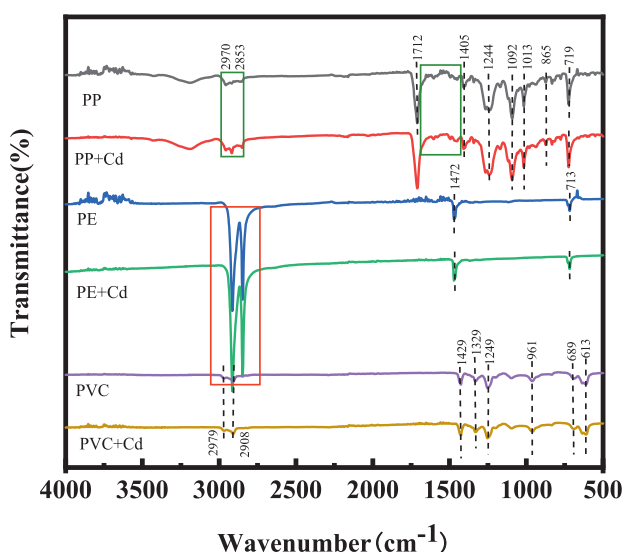
the three MPs spectra before and after adsorption of Cd^{2+} remained nearly unchanged, suggesting that the crystallinity of the MPs before and after the adsorption of Cd^{2+} remained unchanged, and the crystallinity did not affect the adsorption of Cd^{2+} by the MPs. Furthermore, the adsorption of Cd^{2+} by the three MPs was mainly physical adsorption.

Adsorption Kinetics

The adsorption kinetic model of Cd^{2+} by the three MPs is shown in Fig. 6, and the adsorption rate of Cd^{2+} by the MPs is faster at the early stage. At 15 min, the adsorption capacity of the MPs is PP>PVC>PE, but the adsorption capacity of the MPs is PVC>PE>PP at any time in 30 min~1920 min, which is related to the surface structure of the MPs. PP is a small particle detritus-like surface with only a pore structure, while PE and PVC surfaces have folds and protrusions, which may be due to the fast adsorption of Cd^{2+} in PP pores. After 15 minutes, due to the small specific surface area and fewer adsorption sites of PP, the adsorption capacity of PP is less than that of PVC and PE.

The adsorption rate of PP and PE MPs was the maximum in 120 min, and the adsorption rate decreased after 120~960 min, and then the adsorption capacity tended to equilibrate with the increase in time. The adsorption rate of PVC was the maximum in 180 min, and the adsorption rate decreased in 180~960 min, and the adsorption capacity tended to balance with the increase in time. This phenomenon may be due to the rapid migration of metal ions to the surface of the MPs at the initial adsorption, and the adsorption site on the surface of the MPs is occupied, resulting in a gradual weakening of the diffusion rate [23]. In a single system, the adsorption of Cd^{2+} by the MPs reaches adsorption equilibrium in 24 h. During the adsorption equilibrium (1440 min), the adsorption capacity of the MPs to Cd^{2+} was as follows: PVC (0.488 mg/g), >PE (0.373 mg/g),
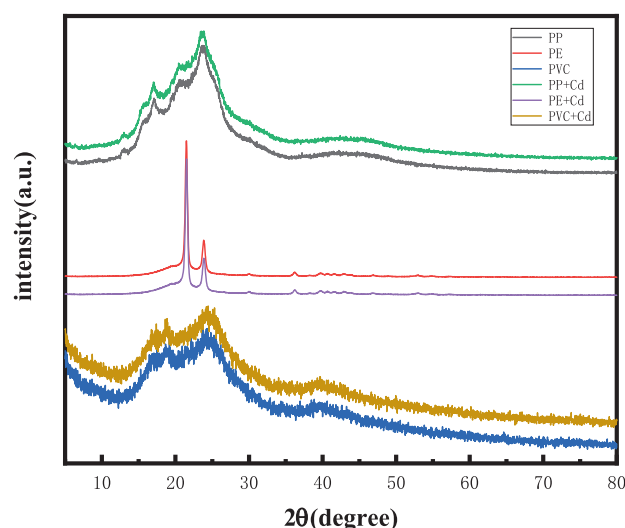

Fig. 4. Fourier infrared spectrum before and after MPs adsorption Cd^{2+}.

Fig. 5. XRD spectra before and after MPs adsorption Cd^{2+}.

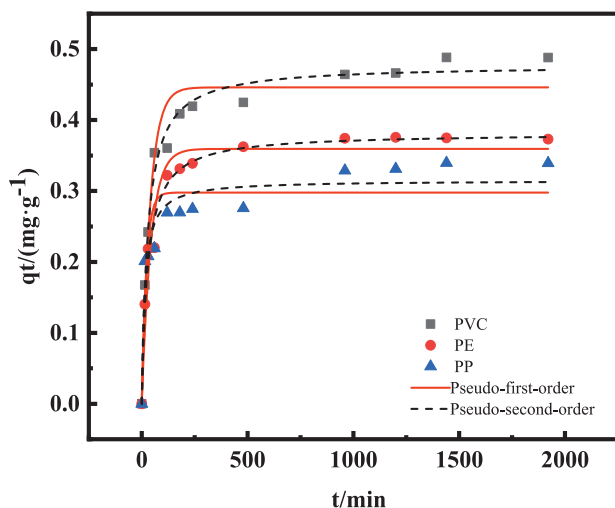Fig. 6. Kinetics of the MPs adsorption of Cd^{2+}.

Fig. 7. Adsorption isothermal diagram of the MPs adsorption Cd^{2+}.

>PP (0.339 mg/g), which indicated that different types of the MPs had different adsorption amounts of Cd^{2+}.

Table 3 lists the parameters for fitting the adsorption of Cd^{2+} by the MPs with the quasi-primary kinetic model (PFO) and quasi-second-order kinetic model (PSO). As depicted in the table, the correlation coefficient of PFO (PVC, PE, PP) R^2 (0.94927~0.83616) was significantly smaller than the correlation coefficient R^2 value of PFO (0.98651~0.92642), and the PSO model could fit better [29], consistent with the results of LV et al. [24]. The above result confirmed that the adsorption of the MPs to Cd^{2+} is a process that affects a variety of effects. Moreover, the equilibrium adsorption capacity of PVC was the largest, and the adsorption capacity of PVC was 25% higher than that of PE and 51% higher than that of PP during adsorption equilibrium. The larger the equilibrium adsorption capacity, the smaller the k_2 value of the MPs, and the smaller the k_2 value, the slower the adsorption rate of the MPs, and the adsorption rate was proportional to the number of occupied points [25].

Adsorption Isothermal

As depicted in Fig. 7, the Freundlich model and the Langmuir model are capable of effectively fitting the adsorption behavior of the MPs to Cd^{2+}. When the concentration of Cd^{2+} was less than 20 mg/L, the adsorption amount of PVC>PE>PP was found at
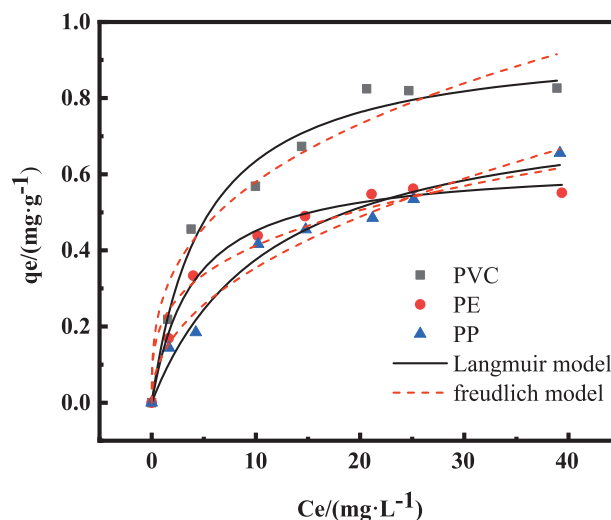
the same concentration. When greater than 20 mg/L, the adsorption amounts of PVC>PP>PE is at equal concentrations. This result may be related to the crystallinity of the MPs; the crystallinity of PE is larger than that of PP and PVC, and it may affect the adsorption effect when the concentration of cadmium is high. The greater the crystallinity, the weaker the adsorption capacity, so the PE adsorption capacity is reduced.

Table 4 lists the parameters of the adsorption of Cd^{2+} by the MPs fitted by the Freundlich model and the Langmuir model. As indicated by the result, the correlation coefficient (PVC, PE, and PP) R^2 (0.97682~0.99276) of the Langmuir model exceeded that of the Freundlich model (PVC, PE, and PP) R^2 (0.94908~0.97430), and MPs were Cd^{2+}. The adsorption process conformed to the Langmuir mode, suggesting that the adsorption of Cd^{2+} by the MPs was mainly the physical adsorption behavior of the monolayer. However, existing research has suggested that when the value of the correlation coefficient R^2 fitted by different models approached or exceeded 0.95, multiple mechanisms was likely to affect the adsorption process [26], and the adsorption process of Cd^{2+} by three MPs The R^2 (0.94908~0.97430) of the Freundlich model reached nearly 0.95, suggesting that the Freundlich model and the Langmuir model can fit the adsorption behavior of the MPs to Cd^{2+}, as reported by Holmes et al. [27]. Both

Table 3. Fitting parameters of kinetic model adsorption of Cd2+ by the MPs.

MPs	Quasi-first-order kinetic equations			Quasi-second-order kinetic equations		
	$k1$/min^{-1}	qe/(mg·g^{-1})	R^2	$k2$/(g·(mg·min)$^{-1}$)	qe/(mg·g^{-1})	R^2
PVC	0.02513	0.44605	0.94927	0.07407	0.47745	0.98651
PE	0.02324	0.35928	0.94896	0.09415	0.38138	0.98355
PP	0.04775	0.29771	0.83616	0.21933	0.31502	0.92042

Table 4. Fitting parameters of adsorption isotherm model for adsorption of Cd^{2+} by the MPs.

MPs	Langmuir adsorption isothermal model			Freundlich adsorption isothermal model		
	qm/(mg·g^{-1})	K_L/(L·mg^{-1})	R^2	K_F/(mg^{1-n}·g^{-1}·L^n)	n	R^2
PVC	0.955676	0.197895	0.97892	0.26779	2.978318	0.95357
PE	0.62964	0.25296	0.99276	0.20962	3.402865	0.94908
PP	0.807272	0.087051	0.97682	0.12246	2.166331	0.97430

Freundlich and Langmuir isotherm models can fully express the adsorption of Cd^{2+} on MPs. The size of the K_L constant in the Langmuir model was correlated with the properties of the adsorbent, primarily expressing the monolayer adsorption on the fixed adsorption site. The larger the value, the stronger the adsorption capacity of the adsorbent will be. As indicated by the maximum K_L value of PVC and the minimum K_L of PP listed in Table 4, the adsorption capacity of PVC was the strongest, consistent with the characterization results of energy spectrum analysis. Freundlich model refers to a nonlinear adsorption model, and MPs adsorption of Cd^{2+} conformed to the Freundlich model, suggesting that adsorption is multi-layer adsorption, n denotes the adsorption index, and the value of n can indicate the size of adsorption strength [28]. If n exceeds 1, the greater the distribution of active sites on the surface of the adsorbent, the greater the adsorption of Cd^{2+} by the MPs will be [32]. As revealed by nonlinear adsorption, the adsorption of Cd^{2+} by the MPs may be affected by electrostatic attraction. In brief, the adsorption of Cd^{2+} by the MPs is the result of the coexistence of monolayer and multilayer adsorption.

Environmental Impact

Effects of Temperature

Fig. 8 shows the comparison of the effects of different temperatures on the adsorption capacities of the three MPs. As indicated by the results, the adsorption capacity of Cd^{2+} for all three MPs was increased with the increase in temperature, and the maximum equilibrium adsorption capacities of PP, PE, and PVC were 0.64, 0.70, and 0.89 mg/g, respectively, at 35ºC. At 15ºC and 35 °C, the equilibrium adsorption capacities of PP and PE were increased by 1.0 time, whereas the equilibrium adsorption capacity of PVC was enhanced by 1.4 times, suggesting that high temperature can facilitate the adsorption process, and the adsorption of the MPs to Cd^{2+} refers to an endothermic reaction. With the increase in the temperature, the entropy value of the system was elevated, the degree of spontaneous reaction of adsorption was up-regulated, and the adsorption capacity of heavy metals was enhanced. Existing research has suggested that temperatures can lead to the change of the crystallinity of the MPs, thus affecting the attraction between adsorbents and heavy metals. With the continuous rise of the temperature,

the equilibrium adsorption capacity at 50ºC declined compared with 35ºC. Li [29] suggested that the increase in the temperature will expedite the movement between molecules to facilitate adsorption, and it can also promote the desorption process, such that the adsorption capacity of the MPs to heavy metals can be reduced. In general, the higher the temperature, the greater the adsorption capacity of the MPs to heavy metals, whereas at higher temperatures (>35ºC), the adsorption capacity was decreased with the increase in the temperature since high temperature will make the movement between molecules faster, thus contributing to the occurrence of desorption. As a result, the equilibrium adsorption capacity of the MPs to heavy metals can be reduced [30].

Effects of pH

Fig. 9 presents the comparison of the effects of the three MPs on the adsorption capacity of Cd^{2+} at pH 3 to 7 values. As indicated by the results, the adsorption capacity of the MPs on Cd^{2+} was also increased with the increase of the pH value, and the effect of the pH value on the adsorption of Cd^{2+} on the three MPs was similar. As depicted in the figure, MPs have the minimum adsorption capacity for Cd^{2+} at pH 3.0, and the three MPs have the maximum adsorption capacity for Cd^{2+} at pH 6.0. At pH 3.0 and 6.0, the adsorption capacity of the MPs to Cd^{2+} increased, and PP, PE, and PVC increased by 1.17, 0.52, and 1 time, respectively. At pH 7.0,
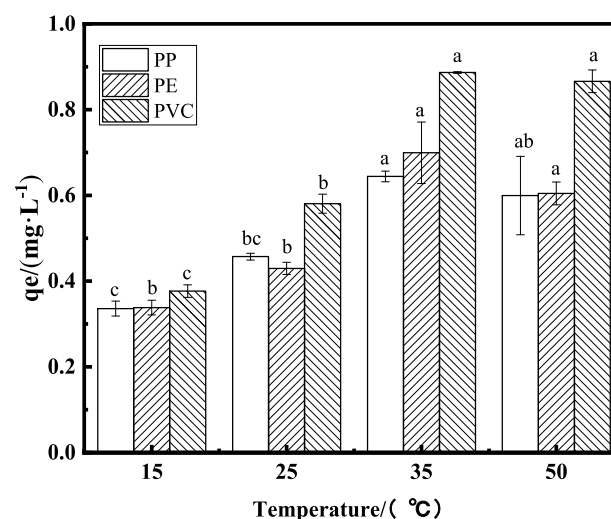
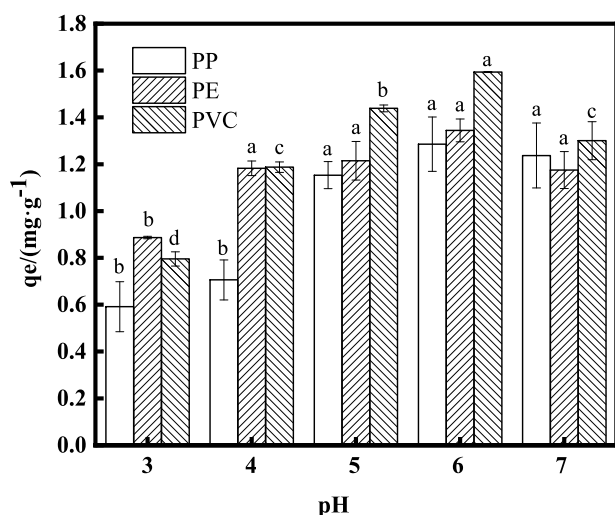Fig. 8. Effect of temperature on adsorption of Cd^{2+} by the MPs.

Fig. 9. Effect of pH on the adsorption of Cd^{2+} by the MPs.

Fig. 10. Effect of salinity on the adsorption of Cd^{2+} in MPs.

the adsorption capacity of the MPs for Cd^{2+} decreases.

The effect of pH value on the adsorption of Cd^{2+} by the MPs has mainly two aspects: it affects the morphology of metal ions in solution; the surface charge density of the MPs and the dissociation of active functional groups affect the adsorption behavior of the MPs to Cd. At low pH, H$^+$ will compete with Cd^{2+} and occupy the adsorption site on the surface of the MPs [31]. With the increase in pH, H$^+$ decreases, the competitive effect weakens, and the amount of the MPs adsorbing Cd^{2+} increases. Therefore, when the pH (3.0~6.0) tended to be increased, the adsorption capacity of the MPs to Cd^{2+} was increased. The functional groups on the surface of the MPs were also deprotonated, thus enhancing their ability to bind to Cd^{2+}. Moreover, the solution's pH was increased, H$^+$ was decreased, and the functional groups were deprotonated [32]. At the pH of 7.0, the adsorption capacity was reduced because CdOH$^+$ was generated at pH 6.0 and Cd(OH)$_2$ precipitation was generated at the pH over 7.0, i.e., the main reason for the decrease in adsorption capacity in an alkaline environment. pH can more significantly affect the surface charge of the MPs. Zeta potential results suggested that the surface of the MPs was negatively charged and Cd^{2+} had a positive charge, such that the two can form complexes through electrostatic attraction to achieve the purpose of adsorption. The effect of the pH value on adsorption capacity was investigated, and the results confirmed that pH value has a greater effect on the adsorption capacity of the MPs since the surface properties of the MPs will change and the morphology of metal ions may also change at different pH values, such that it can affect the Cd^{2+} adsorption capacity on the surface of MPs.

Effects of Salinity

The equilibrium adsorption capacity of Cd^{2+} by the three MPs tended to decline with the increase of Na$^+$ concentration in solutions, decreasing by 3.3 times
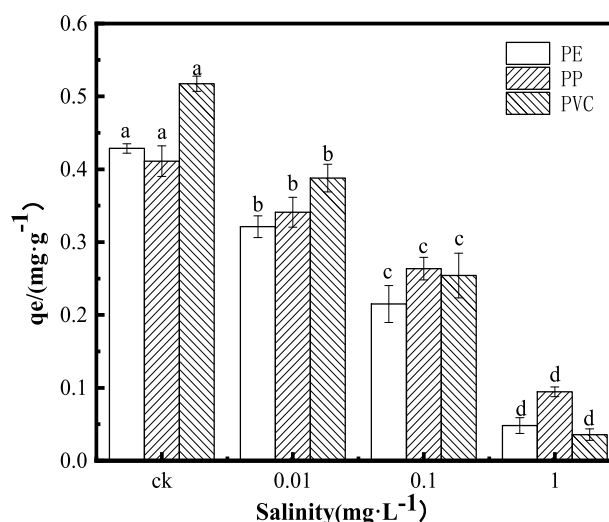
for PP, 8 times for PE, and 13 times for PVC, which was demonstrated by the effect of salt (NaCl) concentration on the adsorption of Cd^{2+} by the MPs (Fig. 10). As revealed by the results, high salinity reduced the adsorption capacity of the MPs on Cd^{2+} and that the effect of the MPs on the equilibrium adsorption capacity of Cd^{2+} at lower salinity was very minimal. The adsorption of heavy metals Cd, Co, and Ni by plastics also declined with an increase in salinity [14], and the results of this study also confirmed the effect of salinity on Cd^{2+} adsorption. The reason for this finding is that MPs compress the electric double layer of the MPs in a high salinity ion environment, such that the attraction between MPs can be reduced and agglomeration behavior will be generated. As a result, the specific surface area, adsorption sites, and adsorption capacity of the clumped-together MPs will be reduced. With the increase in the salinity, the content of Na$^+$ will be increased, and Na$^+$ will compete with Cd^{2+} for adsorption sites, resulting in a lower equilibrium adsorption capacity of the MPs for Cd^{2+} [33, 34]. Moreover, the addition of salinity endows the solution with higher competitiveness and ionic density while reducing the activity and zeta potential of metal ions in solution [35], reducing the release rate of Na$^+$ adsorbed on the surface of the MPs [36], and leading to the lower adsorption capacity for Cd^{2+}, such that the electrostatic attraction between the adsorbent and the adsorbent can be reduced [37]. Furthermore, Tang [38] suggested that the increase in salinity will produce an electrostatic shielding effect between MPs and heavy metals, such that the adsorption of metal ions by the MPs can be reduced.

Conclusion

(1) The equilibrium adsorption capacity of Cd^{2+} was greatest for 13 μm microplastics, and the adsorption

capacity of Cd^{2+} by all three microplastics increased with the reduction in particle size.

(2) The energy intensity of the peaks at 2970~2853 cm^{-1} and 1712~1405 cm^{-1} after PP adsorption of Cd^{2+} varied after adsorption of Cd^{2+} by FTIR, XRD, and EDS energy spectra, and the area of the peak at 2913~2845 cm^{-1} of PE was increased after Cd^{2+} adsorption. However, the energy intensity of the peaks at 2970~2853 cm^{-1} and 1712~1405 cm^{-1} varied after Cd^{2+} adsorption, and the area of the peak at 2913~2845 cm^{-1} of PE varied before and after adsorption. The crystallinity of the three MPs before and after adsorption remained nearly unchanged. Prior to adsorption, no Cd^{2+} was reported, whereas the amounts of Cd^{2+} on the surfaces of PP, PE, and PVC were increased by 0.25% (Wt.), 0.18% (Wt.), and 0.78% (Wt.), respectively, after adsorption.

(3) The adsorption capacity of the MPs on Cd^{2+} followed descending order of PVC>PE>PP, and the adsorption behavior of the MPs on Cd^{2+} was more consistent with the quasi-secondary kinetic equation. The three MPs exhibited the fastest adsorption rate of Cd^{2+} at the early stage while reaching adsorption equilibrium at 24 h. The maximum capacity for Cd^{2+} adsorption on microplastic surfaces was positively correlated with the system-wide concentration of Cd^{2+}. The Cd^{2+} adsorption behavior of the MPs may be explained by the Langmuir and Freundlich models, suggesting that the process of Cd^{2+} adsorption by the MPs can be the consequence of the combined action of monolayer and multilayer adsorption.

(4) External variables salinity , pH, and temperature all affected the Cd^{2+} adsorption capacities of MPs. The equilibrium adsorption capacity of PVC was 34% and 43% greater than that of PP and PE, respectively. The three MPs exhibited their maximum adsorption capacity at 35ºC. At the pH of 6.0, the three MPs' Cd^{2+} adsorption capacities reached their maximum, and PVC's adsorption capacity was elevated by 24% and 18.5% compared with PP and PE, respectively. The equilibrium adsorption of Cd^{2+} by PP, PE, and PVC declined by 3.3, 8 and 13 times, respectively, with the rise of the salt concentration (CK~1 mg·L^{-1}), compared with no salt at a salt concentration of 1 mg/L.

(5) PVC exhibited the strongest Cd^{2+} adsorption capacity of the three MPs, and environmental variables exerted the most significant effect on PVC.

Acknowledgments

Conflict of Interest

All the authors declare having no conflict of interest.

Reference

1. LLORET J., PEDROSA-PAMIES R., VANDAL N., RORTY R., RITCHIE M., MCGUIRE C., CHENOWETH K., VALIELA I. Salt marsh sediments act as sinks for microplastics and reveal effects of current and historical land use changes. Environmental Advances. **4**, 100060, **2021**.
2. WAGNER M., SCHERER C., ALVAREZ-MUN˜OZ D., BRENNHOLT N., BOURRAIN X., BUCHINGER S., FRIES E., GROSBOIS C., KLASMEIER J., MARTI T., RODRIGUEZ-MOZAZ S., URBATZKA R., VETHAAK A.D., WINTHER-NIELSEN M., REIFFERSCHEID G. Microplastics in freshwater ecosystems: What we know and what we need to know. Environmental Sciences Europe. **26** (12), **2014**.
3. RILLIG M.C. Microplastic in terrestrial ecosystems and the soil? Environmental Science & Technology. **46** (12), 6453, **2012**.
4. ALIMI O.S., BUDARZ J.F., HERNANDEZ L.M., TUFENKJI N. Microplastics and nanoplastics in aquatic environments: aggregation, deposition, and enhanced contaminant transport. Environmental Science & Technology. **52** (4), 1704, **2018**.
5. CóZAR A., ECHEVARRíA F., GONZáLEZ-GORDILLO J.I., IRIGOIEN X., ÚBEDA B., HERNáNDEZ-LEóN S., PALAMA Á.T., NAVARRO S., GARCíA-DE-LOMAS J., RUIZ A., FERNáNDEZ-DE-PUELLES M.L., DUARTE C.M. Plastic debris in the open ocean. Proc Natl Acad Sci USA. **111** (28), 10239, **2014**.
6. SUN Y.R., YUAN J.H., ZHOU T., ZHAO Y.C., YU F., MA J. Laboratory simulation of microplastics weathering and its adsorption behaviors in an aqueous environment: A systematic review. Environmental Pollution. **265**, 114864, **2020**.
7. HERNANDEZ L.M., XU E.G., LARSSON H.C.E., TAHARA R., MAISURIA V.B., TUFENKJI N. Plastic teabags release billions of microparticles and nanoparticles into tea. Environmental Science & Technology. **53** (21), 12300, **2019**.
8. LESLIE H.A., VELZEN M.J.M.V., BRANDSMA S.H., VETHAAK A.D., GARCIA-VALLEJO J.J., LAMOREE M.H. Discovery and quantification of plastic particle pollution in human blood. Environment International. **163**, 107199, **2022**.
9. FU J.X., LI Y.A., PENG L., GAO W.X., WANG G.Q. Distinct chemical adsorption behaviors of sulfanilamide as a model antibiotic onto weathered microplastics in complex systems. Colloids and Surfaces A: Physicochemical and Engineering Aspects. **648**, 129337, **2022**.
10. CHEN Z.Y., YANG J.C., HUANG D.Y., WANG S.N., JIANG K., SUN W.M., CHEN Z.H., CAO Z.G., REN Y.H., WANG Q., LIU H.Q., ZHANG X., SUN X.X. Adsorption behavior of aniline pollutant on polystyrene microplastics. Chemosphere. **323**, 138187, **2023**.
11. TANG S., YANG X.Q., ZHANG T., QIN Y.X., CAO C.J., SHI H.H., ZHAO Y.P. Adsorption mechanisms of metal ions (Pb, Cd, Cu) onto polyamide 6 microplastics: New insight into environmental risks in comparison with natural media in different water matrices. Gondwana Research. **110**, 214, **2022**.
12. GODOY V., BLáZQUEZ G., CALERO M., QUESADA L., MARTíN-LARA M.A. The potential of microplastics as carriers of metals. Environmental Pollution. **255**, 113363, **2019**.

13. ALMEIDA C.M.R., MANJATE E., RAMOS S. Adsorption of Cd and Cu to different types of microplastics in estuarine salt marsh medium. Marine Pollution Bulletin. **151**, 110797, **2020**.

14. HOLMES L.A., TURNER A., THOMPSON R.C. Interactions between trace metals and plastic production pellets under estuarine conditions. Marine Chemistry. **167**, 25, **2014**.

15. GUO X., CHEN C., WANG J.L. Sorption of sulfamethoxazole onto six types of microplastics. Chemosphere. **228**, 300, **2019**.

16. WANG L.L., GUO C.X., QIAN Q.Q., LANG D.N., WU R.L., ABLIZ S., WANG W., WANG J. Adsorption behavior of UV aged microplastics on the heavy metals Pb(II) and Cu(II) in aqueous solutions. Chemosphere. **313**, 137439, **2023**.

17. CHEN Y.A., QIAN Y.K., SHI Y.J., WANG X.Y., TAN X., AN D. Accumulation of chiral pharmaceuticals (ofloxacin or levofloxacin) onto polyethylene microplastics from aqueous solutions. Science of the Total Environment. **823**, 153765, **2022**.

18. YUAN W.K., ZHOU Y.F., CHEN Y.L., LIU X.N., WANG J. Toxicological effects of microplastics and heavy metals on the Daphnia magna. Science of the Total Environment. **746**, 141254, **2020**.

19. HIDAYAT D., PURWANTO A., WANG W.N., OKUYAMA K. Preparation of size-controlled tungsten oxide nanoparticles and evaluation of their adsorption performance. Materials Research Bulletin. **45** (2), 165, **2010**.

20. WU P.F., CAI Z.W., JIN H.B., TANG Y.Y. Adsorption mechanisms of five bisphenol analogues on PVC microplastics. Science of the Total Environment. **650** (Part 1), 671, **2018**.

21. ZHOU Y.F., YANG Y.Y., LIU G.H., HE G., LIU W.Z. Adsorption mechanism of cadmium on microplastics and their desorption behavior in sediment and gut environments: The roles of water pH, lead ions, natural organic matter and phenanthrene. Water Research. **184**, 116209, **2020**.

22. WANG F.Y., YANG W.W., CHENG P., ZHANG S.Q., ZHANG S.W., JIAO W.T., SUN Y.H. Adsorption characteristics of cadmium onto microplastics from aqueous solutions. Chemosphere. **235**, 1073, **2019**.

23. FAN C.Z., LI K., LI J.X., YING D.W., WANG Y.L., JIA J.P. Comparative and competitive adsorption of Pb(II) and Cu(II) using tetraethylenepentamine modified chitosan/CoFe$_2$O$_4$ particles. Journal of Hazardous Materials. **326**, 211, **2017**.

24. LV M.J., ZHANG T., YA H.B., XING Y., WANG X., JIANG B. Effects of heavy metals on the adsorption of ciprofloxacin on polyethylene microplastics: Mechanism and toxicity evaluation. Chemosphere. **315**, 137745, **2023**.

25. WANG Q.J., ZHANG Y., WANGJIN X.X., WANG Y.L., MENG G.H., CHEN Y.H. The adsorption behavior of metals in aqueous solution by microplastics effected by UV radiation. Journal of Environmental Sciences. **87**, 272, **2020**.

26. GAO X., HASSAN I., PENG Y.T., HUO S.L., LING L. Behaviors and influencing factors of the heavy metals adsorption onto microplastics: A review. Journal of Cleaner Production. **319**, 128777, **2021**.

27. HOLMES L.A., TURNER A., THOMPSON R.C. Adsorption of trace metals to plastic resin pellets in the marine environment. Environmental Pollution. **160**, 42, **2012**.

28. YAN J., GONG J.L., ZENG G.M., SONG B., ZHANG P., LIU H.Y., HUAN S.Y., LI X.D. Carbon nanotube-impeded transport of non-steroidal anti-inflammatory drugs in Xiangjiang sediments. Journal of Colloid and Interface Science. **498**, 229, **2017**.

29. LI Y.H., ZHANG Y., SU F., WANG Y.Y., PENG L.L., LIU D. Adsorption behaviour of microplastics on the heavy metal Cr(VI) before and after ageing. Chemosphere. **302**, 134865, **2022**.

30. LI H.Q., HUANG G.H., AN C.J., HU J.T., YANG S.Q. Removal of tannin from aqueous solution by adsorption onto treated coal fly ash: kinetic, equilibrium, and thermodynamic studies. Industrial & Engineering Chemistry Research. **52** (45), 15923, **2013**.

31. RUZIWA D., CHAUKURA N., GWENZI W., PUMURE I. Removal of Zn^{2+} and Pb^{2+} ions from aqueous solution using sulphonated waste polystyrene. Journal of Environmental Chemical Engineering. **3** (Part A), 2528, **2015**.

32. QIU H., NI W.X., ZHANG H.H., CHEN K., YU J.C. Fabrication and evaluation of a regenerable HFO-doped agricultural waste for enhanced adsorption affinity towards phosphate. The Science of the Total Environment. **703**, 135493, **2020**.

33. LIU G.Z., ZHU Z.L., YANG Y.X., SUN Y.R., YU F., MA J. Sorption behavior and mechanism of hydrophilic organic chemicals to virgin and aged microplastics in freshwater and seawater. Environmental Pollution. **246**, 26, **2019**.

34. LI J., ZHANG K.N., ZHNAG H. Adsorption of antibiotics on microplastics. Environmental Pollution. **237**, 460, **2018**.

35. HAN Y.T., CAO X., OUYANG X., SOHI S.P., CHEN J.W. Adsorption kinetics of magnetic biochar derived from peanut hull on removal of Cr (VI) from aqueous solution: Effects of production conditions and particle size. Chemosphere. **145**, 336, **2016**.

36. BARUS B.S., CHEN K., CAI M.G., LI R.M., CHEN H.R., LI C., WANG J., CHENG S.Y. Heavy metal adsorption and release on polystyrene particles at various salinities. Frontiers in Marine Science. **8**, 671802, **2021**.

37. FILIUS J.D., LUMSDAN D.G., MEEUSSEN J.C.L., HIEMSTRA T., RIEMSDIJK W.H.V. Adsorption of fulvic acid on goethite. Geochimica et Cosmochimica Acta. **64** (1), 51, **2000**.

38. TANG S., LIN L.J., WANG X.S., YU A.Q., SUN X. Interfacial interactions between collected nylon microplastics and three divalent metal ions (Cu(II), Ni(II), Zn(II)) in aqueous solutions. Journal of Hazardous Materials. **403**, 123548, **2020**.